Environmental Science and Ecotechnology 11 (2022) 100186

Contents lists available at ScienceDirect

Environmental Science and Ecotechnology

journal homepage: www.journals.elsevier.com/environmental-science-and-ecotechnology/

Original Research

A tartrate-EDTA-Fe complex mediates electron transfer and enhances ammonia recovery in a bioelectrochemical-stripping system

De-Xin Zhang [a, b, 1], Si-Yuan Zhai [a, 1], Ran Zeng [a, c], Cheng-Yan Liu [a, b], Bo Zhang [a], Zhe Yu [a, b], Li-Hui Yang [a], Xi-Qi Li [d], Ya-Nan Hou [e], Ai-Jie Wang [a, b, d], Hao-Yi Cheng [d, *]

[a] Key Laboratory of Environmental Biotechnology, Research Center for Eco-Environmental Sciences, Chinese Academy of Sciences, Beijing, 100085, China
[b] University of Chinese Academy of Sciences, Beijing, 100049, China
[c] College of Civil Engineering, Nanjing Tech University, Nanjing, 211816, China
[d] State Key Lab of Urban Water Resource and Environment, School of Civil and Environmental Engineering, Harbin Institute of Technology Shenzhen, Shenzhen, 518055, PR China
[e] Tianjin Key Laboratory of Aquatic Science and Technology, School of Environmental and Municipal Engineering, Tianjin Chengjian University, Tianjin, 300384, China

ARTICLE INFO

Article history:
Received 19 February 2022
Received in revised form
13 May 2022
Accepted 13 May 2022

Keywords:
Bioelectrochemical system
Ammonia recovery
Electron mediator
Stripping
Tartrate-EDTA-Fe

ABSTRACT

Traditional bioelectrochemical systems (BESs) coupled with stripping units for ammonia recovery suffer from an insufficient supply of electron acceptors due to the low solubility of oxygen. In this study, we proposed a novel strategy to efficiently transport the oxidizing equivalent provided at the stripping unit to the cathode by introducing a highly soluble electron mediator (EM) into the catholyte. To validate this strategy, we developed a new kind of iron complex system (tartrate-EDTA-Fe) as the EM. EDTA-Fe contributed to the redox property with a midpoint potential of −0.075 V (vs. standard hydrogen electrode, SHE) at pH 10, whereas tartrate acted as a stabilizer to avoid iron precipitation under alkaline conditions. At a ratio of the catholyte recirculation rate to the anolyte flow rate (R_{C-A}) of 12, the NH_4^+-N recovery rate in the system with 50 mM tartrate-EDTA-Fe complex reached 6.9 ± 0.2 g N m^{-2} d^{-1}, approximately 3.8 times higher than that in the non-EM control. With the help of the complex, our system showed an NH_4^+-N recovery performance comparable to that previously reported but with an extremely low R_{C-A} (0.5 vs. 288). The strategy proposed here may guide the future of ammonia recovery BES scale-up because the introduction of an EM allows aeration to be performed only at the stripping unit instead of at every cathode, which is beneficial for the system design due to its simplicity and reliability.

© 2022 The Authors. Published by Elsevier B.V. on behalf of Chinese Society for Environmental Sciences, Harbin Institute of Technology, Chinese Research Academy of Environmental Sciences. This is an open access article under the CC BY-NC-ND license (http://creativecommons.org/licenses/by-nc-nd/4.0/).

1. Introduction

In recent years, bioelectrochemical systems (BESs) have been widely studied in fields in which "clean products", including electricity, biogas (CH_4 and H_2) [1], and industrial and agricultural materials, are recovered. Nitrogen is one of the key nutrients and contaminants in diverse types of wastewaters [2], such as domestic wastewater, industrial wastewater, urine, manure, digestate, reject water, black water, and landfill leachate. A high concentration of ammonia nitrogen can be effectively recovered using a BES coupled with a recovery unit (e.g., stripping and membrane-based absorption). In this integrated system, ammonium ions are transported from the anode chamber to the cathode chamber via current-driven migration [3,4] and then converted to free ammonia under high pH conditions in the cathode chamber [5–7]. With the assistance of the recovery unit, free ammonia can be finally recovered as a high-purity ammonium salt [8–10]. Compared to traditional ammonia recovery techniques, BESs are considered to be more sustainable and cost effective because they do not require chemical additives and consume less or even produce energy.

The separation of free ammonia from the catholyte in an early BES for ammonia recovery was performed by direct stripping in a cathode chamber [11]. In this system, aeration not only provided

* Corresponding author. School of Civil and Environmental Engineering, Harbin Institute of Technology Shenzhen, Shenzhen, 518055, China.
E-mail address: chenghaoyihit@126.com (H.-Y. Cheng).
[1] Both authors contributed equally to this work.

https://doi.org/10.1016/j.ese.2022.100186
2666-4984/© 2022 The Authors. Published by Elsevier B.V. on behalf of Chinese Society for Environmental Sciences, Harbin Institute of Technology, Chinese Research Academy of Environmental Sciences. This is an open access article under the CC BY-NC-ND license (http://creativecommons.org/licenses/by-nc-nd/4.0/).

oxygen for the cathodic reaction but also acted as a source of stripping gas. Subsequently, the system was further improved by integrating the cathode chamber with an individual stripping column by recirculating the catholyte [3,12], which therefore resulted in a much higher stripping efficiency (over 90%) [13]. Notably, if the aeration point is moved from the cathode chamber to the stripping column, the ammonia recovery rate would be limited if catholyte recirculation is not performed at a sufficiently high rate to provide sufficient dissolved oxygen (DO). However, because the water solubility of oxygen is very poor (~8 mg L^{-1}), the ratio of the catholyte recirculation rate to the flow rate of ammonium-containing wastewater is likely far from acceptable in practice. For example, to remove 1 g NH_4^+-N L^{-1} at the anode, this ratio has to be at least 70, even assuming 100% current efficiency for ammonium migration from the anode chamber to the cathode chamber. Additionally, the high-strength recirculation rate leads to a high flow rate of the stripping gas and therefore increases the capital and operation costs of the entire stripping-absorption system. Although adding another aeration point in the cathode chamber could be a solution, this strategy can complicate the system design because the ammonia-containing gas leaving the cathode chamber must also be connected to the absorption system through a well-sealed tubing network. This might not be a major issue for lab-scale systems, which usually have only one cathode chamber. Regarding the system scale-up for engineering applications, there could be hundreds or even more cathode chambers due to the commonly employed stack and modularization design for BESs [14,15]. Performing aeration and collecting the gas at every single cathode chamber is costly and unreliable.

Here, we propose a novel strategy in which a certain readily soluble electron mediator (EM) is introduced into the catholyte (schematically illustrated in Fig. 1). The principle of this strategy is that the oxidized EM is converted to its reduced form at the cathode, producing a current and driving ammonium transportation. The reduced EM is then reoxidized by air in the stripping column, where the separation of ammonia occurs simultaneously. Because the EM is highly soluble, the oxidized EM could provide a much higher concentration of the oxidizing equivalent for the cathodic reaction compared to DO. Therefore, a high ammonia recovery rate would be achieved at a much lower catholyte recirculation rate. To achieve this goal, the selected EM is expected to have the following properties: (i) the solubility of the EM should be at least 2 orders of magnitude higher than that of DO, (ii) the reduction potential of the oxidized EM under alkaline conditions (i.e., free ammonia needs to be predominant in the total ammonia at pH = 10 as an example) should be more positive than the bioanode potential to allow spontaneous current generation, (iii) the reduced EM generated at the cathode can be readily oxidized back to its oxidized form by oxygen, (iv) the EM should be stable under alkaline conditions and not diffuse into the anode chamber, and (v) the EM should be readily accessible and inexpensive.

In this proof-of-concept work, the proposed system, which is shown in Fig. 2, was simplified by constructing the BES as a minimal unit (one anode chamber coupled with one cathode chamber). EDTA-Fe(III)/Fe(II) was selected as a model EM because the properties of this redox couple (as shown in Table 1) [16–19] likely meet most of the requirements mentioned above. Moreover, previous BES studies showed that under electron acceptor nonlimiting conditions, using EDTA-Fe(III) as an electron acceptor at a graphite electrode (which is inexpensive because a noble metal catalyst is not used) could generate a higher current than using oxygen, suggesting its superior dynamic performance [18]. To improve the stability of EDTA-Fe(III) under alkaline conditions, tartrate, which is known to form a stable iron chelate at pH values of up to 11, could be introduced [20].

The aims of this study are to (i) explore the stability and redox behavior of the tartrate-EDTA-Fe complex under alkaline conditions and (ii) demonstrate that the employment of tartrate-EDTA-Fe in the catholyte could promote ammonia recovery and reduce the recirculation rate of the catholyte with only one aeration point in the stripping column. This study sheds light on the scale-up of ammonia recovery BESs with a much simpler system design.

2. Materials and methods

2.1. Setup of the ammonia recovery system and the design of different cathode modes

The ammonia nitrogen recovery system consisted of a two-chamber bioelectrochemical system (120 mL working volume for the anode chamber, 180 mL working volume for the cathode chamber) and an ammonia stripping-absorption unit. The anode and cathode chambers were separated by a cation exchange membrane (CEM, 12 cm × 8 cm; CMI-7000, Membranes International, USA). Four custom-made carbon brushes (height 10 cm, diameter 2 cm) [21] were employed and connected in parallel to form the anode, and another four were used as the cathode in the same way. The anode and cathode were connected to a 10 Ω

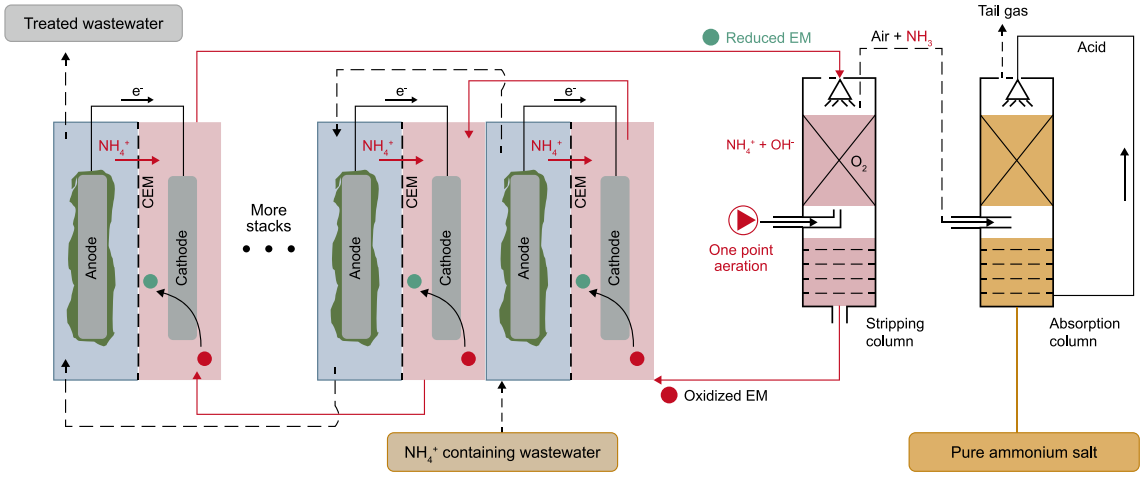

Fig. 1. Schematic diagram of the proposed ammonia recovery strategy with an electron mediator (EM)-amended catholyte.

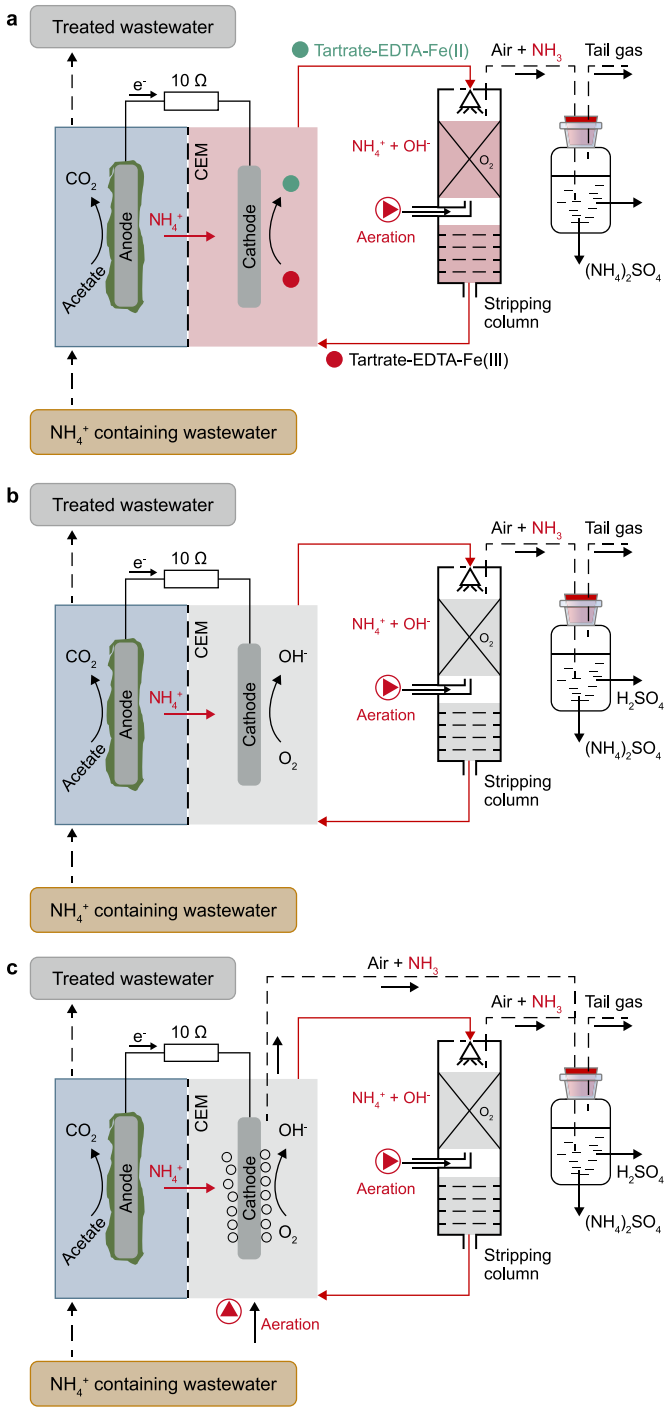

Fig. 2. Schematic diagram of the ammonia recovery systems with different cathode modes in this work: **a**, $S_{EM\text{-}1A}$; **b**, $S_{NonEM\text{-}1A}$; **c**, $S_{NonEM\text{-}2A}$.
Abbreviations: EM and NonEM refer to the presence and absence of an electron mediator in the catholyte. 1A refers to one aeration point in the stripping column, and 2A refers to two aeration points in the stripping column and cathode chamber.

resistance in series, which was used to monitor the current. Two Ag/AgCl reference electrodes (saturated KCl, 197 mV vs. standard hydrogen electrode, SHE) were placed in the anode and cathode chambers to measure the corresponding electrode potentials. The BES was equipped with a multichannel data logger (Model 2700, Keithley Instruments Inc., USA) to record the output current and electrode potentials. The ammonia stripping-absorption unit consisted of one stripping column (height 0.8 m, diameter 0.04 m) filled with pall rings (packing height 0.3 m) and one absorption bottle filled with 500 mL 0.5 M H_2SO_4. The diameter, height and thickness of each pall ring were 16 mm, 16 mm, and 1.1 mm, respectively. The gas–liquid ratio in the stripping column (ratio of the aeration flow rate to the catholyte recirculation rate) was set to 500.

To better understand the role of tartrate-EDTA-Fe in enhancing ammonia removal and recovery, three different cathode modes were designed and are illustrated in Fig. 2. Fig. 2a shows the BES reactor coupled with the ammonia stripping-absorption unit via the recirculation of the tartrate-EDTA-Fe-amended catholyte between the cathode chamber and stripping column. In this case, just one aeration point was placed at the bottom of the stripping column. The setup with this kind of cathode mode was denoted $S_{EM\text{-}1A}$ (reactor with electron mediator and 1-point aeration). The control, $S_{NonEM\text{-}1A}$, had the same setup as $S_{EM\text{-}1A}$ but only used the NaCl catholyte without the EM (Fig. 2b). Another control without the EM was employed, but it was modified by adding a second aeration point to the cathode chamber to ensure a sufficient oxygen supply for the cathodic reaction ($S_{NonEM\text{-}2A}$). Because aeration in the cathode chamber can also remove ammonia from the catholyte, an additional gas collection tube was used to connect the head space of the cathode chamber to the absorption bottle (Fig. 2c).

2.2. Operations of the ammonia recovery systems

Three BES reactors were started up in parallel in the cathode mode $S_{NonEM\text{-}1A}$. The effluent of a steady-operated microbial fuel cell that was fed acetate was employed as the inoculum and was volumetrically (1:1) mixed with synthetic ammonium wastewater (50 mM PBS, 1700 mg L^{-1} sodium acetate, 450 mg L^{-1} NH_4^+-N, 10 mL L^{-1} Wolf's mineral and 10 mL L^{-1} vitamin solution), and the mixture was continuously fed into the anode chamber of the BES reactors at a flow rate of 10 mL h^{-1}. A 50 mM NaCl solution was used as the catholyte, which continuously recirculated between the cathode chamber and the stripping column. The ratio of the catholyte recirculation rate to the anolyte flow rate ($R_{C\text{-}A}$) was set to 12. The aeration flow rate was set to 1 L min^{-1}. After two days of operation, the anode feed was switched to the synthetic ammonium wastewater alone. When a stable output current was observed for a few days, the start-up of the BES was considered to be finished.

Subsequently, the operation of one of the three reactors was kept in the cathode mode $S_{NonEM\text{-}1A}$, whereas the other two reactors were switched to the cathode modes $S_{EM\text{-}1A}$ and $S_{NonEM\text{-}2A}$. The catholytes of $S_{NonEM\text{-}1A}$ and $S_{NonEM\text{-}2A}$ were renewed by a 50 mM NaCl solution, whereas that of $S_{EM\text{-}1A}$ was replaced by a 50 mM tartrate-EDTA-Fe solution. For $S_{NonEM\text{-}2A}$, the aeration flow rates in the stripping column and in the cathode chamber were set to 1 L min^{-1} and 0.2 L min^{-1}, respectively. Synthetic ammonium wastewater was fed into the anode chamber at an identical flow rate of 10 mL h^{-1} in all the systems. First, the ammonium removal and recovery performances of the reactors with different cathode modes were compared by setting $R_{C\text{-}A}$ to 12.0 for each reactor. Then, the performance of $S_{EM\text{-}1A}$ was further investigated by varying $R_{C\text{-}A}$ (0.5, 1.0, and 6.0). All of the experiments mentioned above were conducted at room temperature.

2.3. Cyclic voltammetry

The redox reversibility of tartrate-EDTA-Fe was characterized by cyclic voltammetry (CV) in a standard three-electrode electrolytic cell system. The working, counter and reference electrodes were glassy carbon, platinum wire mesh (10 mm × 10 mm), and Ag/AgCl

Table 1
Properties of EDTA-Fe.

Properties	Notes	References
Water solubility	Up to 200 mM, which is about three orders of magnitude higher than that of oxygen	[16]
Redox potential	52 mV at pH 8 with a negative shift of 44 mV pH^{-1} under alkaline conditions	[17]
Oxidation rate with oxygen	The reduced form is readily oxidized to its oxidized form by oxygen under alkaline conditions	[18]
Stability under alkaline conditions	Not stable and tends to form a hydroxy Fe precipitate	[18]
Accessibility and cost	Widely used in diverse industries and low cost (approximately $1.05[a] per mol)	[19]

[a]: Price is available at www.alibaba.com (accessed on Feb. 19th, 2022).

electrodes, respectively. The glassy carbon electrode was polished with Al_2O_3 before use, and then the electrode polishing degree was tested with a 5 mM potassium ferricyanide and 0.2 M potassium chloride mixed solution [22]. The potential windows were −1.0–0.6 V (vs. Ag/AgCl) and −1.2–0.4 V under neutral and alkaline conditions, respectively. All CV tests were conducted at a scan rate of 5.0 mV s^{-1} using a potentiostat (model-660D, CHI Instruments Inc., Shanghai, China).

2.4. Chemical analysis

The anolyte and catholyte samples were collected and filtered through filters (0.45 μm) before measurement. The ammonia nitrogen concentration was analyzed using the Nessler reagent colorimetry method [23]. The chemical oxygen demand (COD) was determined using a HACH rapid test reagent tube (High range, 20–1500 mg L^{-1}) with a HACH spectrophotometer (DR6000, HACH, USA). The dissolved iron concentration was detected with inductively coupled plasma optical emission spectroscopy (OPTIMA 8300, PerkinElmer Co., USA). Dissolved oxygen (DO) was determined using a portable multiparameter measuring instrument (Multi 3420, WTW, Germany).

2.5. Calculations

Relevant calculations are described in Text S1.

3. Results and discussion

3.1. Alkaline stability and redox behavior of the tartrate-EDTA-Fe complex

The alkaline stability of tartrate-EDTA-Fe was investigated with different molar ratios of tartrate to EDTA-Fe (0, 0.2, 0.25, 0.3, 0.5, and 1.0) at pH 10. In the absence of tartrate, Fe loss was detected during the 2-min solution preparation (Fig. 3a), and the turbidity was directly observed during the EDTA-Fe preparation process. In contrast, the measured total dissolved Fe (Fe_{Total}) concentration in the tartrate-EDTA-Fe complex was basically consistent with the theoretical value of added Fe when the solution was just mixed. However, Fe loss still occurred in the tartrate-EDTA-Fe complex after 140 h when the molar ratio of tartrate to EDTA-Fe was lower than 0.33. The Fe_{Total} concentration was reduced to 42.64 ± 0.45 mM and 44.82 ± 0.09 mM when the molar ratio of tartrate to EDTA-Fe was 0.2 and 0.25, respectively. Significantly, the Fe_{Total} concentrations were basically the same as the initial value when more tartrate was added, and almost no precipitation was visible in the EDTA-Fe-tartrate system. The resulting iron loss was consistent with the solution turbidity after 140 h, indicating that it may be caused by the hydrolysis of iron and formation of an iron hydroxide [18]. The above results suggested that tartrate acts as a stabilizer in the EDTA-Fe(III) complex system, which is conducive to the formation of stable iron chelates. In the following experiments, the tartrate/EDTA-Fe molar ratio was set as 1.0 to ensure that EDTA-Fe was stable under alkaline conditions.

Cyclic voltammetry was employed to understand the redox behavior of the tartrate-EDTA-Fe complex under alkaline conditions (pH = 10). The result was compared with either the EDTA-Fe complex alone or the tartrate-Fe complex alone. As shown in Fig. 4a, a pair of reversible peaks appeared in the CV spectrum of the tartrate-EDTA-Fe complex, with the reduction peak, oxidation peak and midpoint potentials at −0.157 V, 0.007 V, and −0.075 V, respectively. A similar CV curve was observed in the test with the EDTA-Fe complex, whereas the CV of the tartrate-Fe complex showed an irreversible reduction peak with a much more negative potential (−0.776 V). These results indicated that the redox behavior of the tartrate-EDTA-Fe complex is mainly due to EDTA-Fe. Notably, the BESs used to recover ammonia in this study were operated in microbial fuel cell mode. Thus, the cathode potential would be more positive than the bioanode potential (at least higher than the oxidation potential of acetate, −0.28 V vs. SHE [23]). For this reason, although a reduction peak was observed in the CV of the tartrate-Fe complex, the onset potential appeared too negative for it to contribute to the electrochemical reduction of Fe(III) in the following ammonia recovery test. To further elucidate the redox peaks in the CV of the tartrate-EDTA-Fe complex obtained under alkaline conditions, a CV test was also conducted at pH 7, and the corresponding voltammograms showed a pair of redox peaks with a midpoint potential of 0.058 V (vs. SHE) (Fig. S1). A comparison of the midpoint potentials obtained at pH 10 and pH 7 revealed a negative shift of 0.133 V (or 0.044 V per unit pH increase). Previously, it was reported that the midpoint potential of the EDTA-Fe complex underwent a negative shift of 0.044 V pH^{-1} in the CVs obtained at pH > 6.8, which was suggested to result from the electrochemical redox reaction of the hydroxide form of EDTA-Fe(III)/Fe(II) [17]. Because EDTA-Fe was suggested to govern the redox behavior as mentioned above, the redox peaks of the tartrate-EDTA-Fe complex observed at pH 10 may follow the same rule.

The CV results clearly showed that the redox reaction of the tartrate-EDTA-Fe complex is electrochemically reversible. However, in our proposed BES-stripping system, the actual redox process would be not the same but would involve coupled processes, namely, the electrochemical reduction of tartrate-EDTA-Fe(III) at the cathode and its reoxidation by oxygen in the stripping column. To model this process, a chronoamperometry test was conducted at −0.2 V in the BES reactor to reduce tartrate-EDTA-Fe(III) in the cathode chamber. As shown in Fig. S2, a current of approximately 23 mA was generated initially, and then it gradually decreased to almost zero after 60 h. The accumulated charge in 67 h was calculated to be as 964.94 C, which was consistent with the value (902.71 C) calculated based on Fe(III) conversion to Fe(II) (46.78 mM). Then, the reduced tartrate-EDTA-Fe solution was removed to perform aeration in a baker. As shown in Fig. 4b, tartrate-EDTA-Fe(II) was rapidly reoxidized in 2 h. These results clearly suggested that the tartrate-EDTA-Fe complex is a suitable electron mediator that can

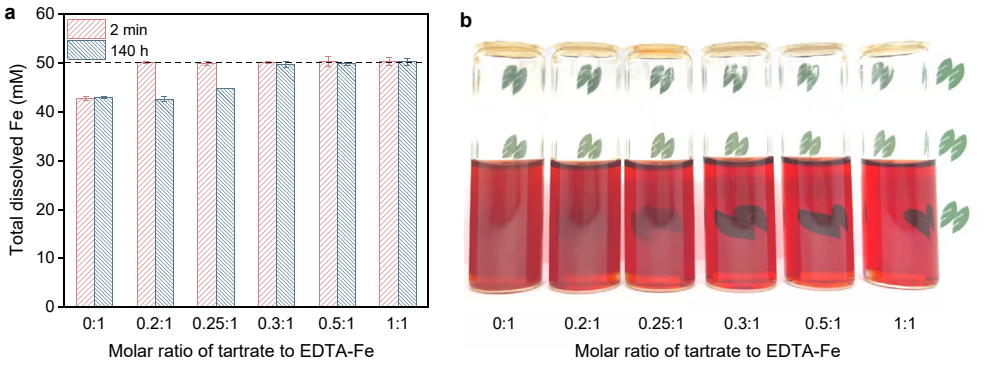

Fig. 3. **a**, Total dissolved Fe concentrations detected 2 min and 140 h after catholyte preparation with different molar ratios of tartrate to EDTA-Fe (under alkaline conditions, total Fe = 50 mM). **b**, Corresponding photo of the iron complex solutions collected after 140 h.

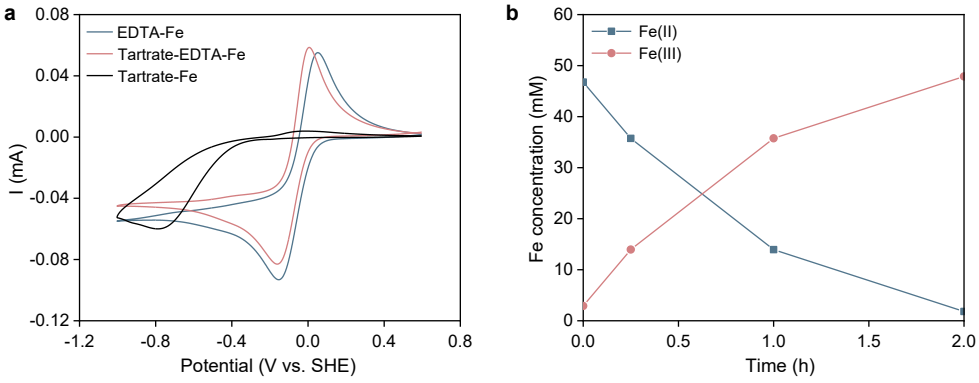

Fig. 4. **a**, Cyclic voltammograms of tartrate-EDTA-Fe, EDTA-Fe and tartrate-Fe at pH 10 (50 mM, scan rate: 5.0 mV s^{-1}). **b**, Variations in Fe(II) and Fe(III) in a tartrate-EDTA-Fe solution (50 mM) under aeration at a 1 L min^{-1} flow rate of air (the tartrate-EDTA-Fe solution was first reduced in the BES reactor at a cathode potential of −0.2 V vs. SHE, see Fig. S2).

transport the oxidizing equivalent from oxygen to the BES cathode.

3.2. Performance of the ammonia recovery system in different cathode modes

3.2.1. Current profiles

At the start-up stage, all three BES reactors were operated in the same cathode mode, $S_{NonEM\text{-}1A}$ (no tartrate-EDTA-Fe in the catholyte and one-point aeration in the stripping column). After inoculation, the variations in the currents in all the BESs followed a similar trend, gradually increasing in the first 48 h and then remaining at approximately 0.270 ± 0.004 A m^{-2} (Fig. 5a). This observation indicated that the acclimated bioanodes in all the BES reactors had similar electricity-generation capabilities. Subsequently, the BES reactors were operated in different cathode modes to compare the current generation performances.

When another aeration point was added to the cathode chamber ($S_{NonEM\text{-}2A}$), an obvious increase in the current density relative to that of $S_{NonEM\text{-}1A}$ was observed (0.883 ± 0.004 A m^{-2} vs. 0.270 ± 0.004 A m^{-2}, Fig. 5a), indicating that the limited current output observed when aeration was only performed in the stripping column was due to the insufficient supply of an electron acceptor (oxygen). We also calculated the supply rate of the oxidizing equivalent in $S_{NonEM\text{-}1A}$ to be 10.28 C h^{-1} based on the catholyte recirculation rate (0.12 L h^{-1}), and the measured dissolved oxygen in the catholyte was saturated (~7.1 mg L^{-1}) in the catholyte coming out of the stripping column. We found that this value was very close to the consumption rate of the oxidizing equivalent (9.36 C h^{-1}) determined from the current (2.6 mA), which therefore supported the conclusion that the supply of electron acceptors in $S_{NonEM\text{-}1A}$ was insufficient.

When the tartrate-EDTA-Fe-amended catholyte ($S_{EM\text{-}1A}$) was used, the current density initially increased to approximately 1.5 A m^{-2}, then gradually decreased and stabilized at 1.20 ± 0.02 A m^{-2} (Fig. 5a). When the catholyte was replaced by the tartrate-EDTA-Fe complex, the concentration of Fe(III) was relatively high at the beginning, and a correspondingly higher current density was obtained due to more abundant electron acceptors. As the redox reaction of iron reached a dynamic equilibrium, the generated current density reached a stable state. The much higher current density obtained in the stable state was attributed to the sufficient supply rate of the oxidizing equivalent in $S_{EM\text{-}1A}$ (579 C h^{-1}), which was estimated to be 50 times higher than that in $S_{NonEM\text{-}1A}$. Under this condition, the consumption rate of the oxidizing equivalent calculated based on the generated current (~11.5 mA) was 41.4 C h^{-1}, which was significantly lower than the supply rate, clearly suggesting that the introduction of the tartrate-EDTA-Fe complex overcame the limitation in the oxidizing equivalent supply. Compared with the current density of $S_{NonEM\text{-}2A}$, which was also not limited by the oxidizing equivalent supply, the current density of $S_{EM\text{-}1A}$ was still found to be 36% higher. For $S_{NonEM\text{-}2A}$, the cathode working potential was measured to be -0.103 ± 0.020 V (Fig. 5b), which was much more negative than the theoretical reduction potential of oxygen at pH 10 (0.627 V vs. SHE) [24], indicating that oxygen reduction at the cathode suffered from slow kinetics. This was not surprising because the cathode material used in this work was just a plain carbon fiber that was not modified by a catalyst, such as platinum, which is known to be important for

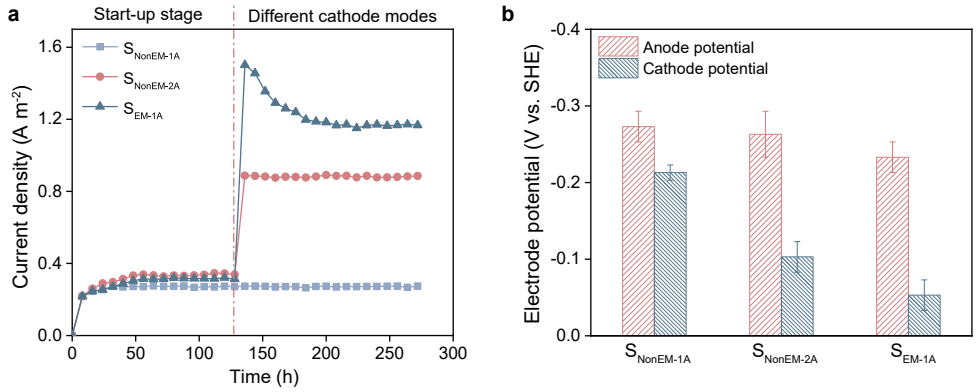

Fig. 5. Electrochemical performances of systems operated in different cathode modes: **a**, current densities; **b**, electrode potentials of the anode and cathode.

overcoming the kinetic barrier of the electrochemical reduction of oxygen. In contrast, the electrochemical reduction of tartrate-EDTA-Fe(III) appeared to be highly efficient, as indicated by its small overpotential (0.103 V calculated by subtracting the cathode working potential, -0.053 ± 0.020 V in Fig. 5b, from the onset potential of the reduction peak in the CV, approximately 0.050 V in Fig. 4a). As a result, the cathode working potential in $S_{EM\text{-}1A}$ was -0.053 ± 0.020 V more positive than that in $S_{NonEM\text{-}2A}$ and therefore provided a higher driving force to promote current generation.

3.2.2. NH_4^+-N removal and recovery

Prior to investigating the NH_4^+-N removal and recovery performance, the catholytes and absorption solutions were renewed. As shown in Fig. 6a, the total ammonia nitrogen (TAN) initially accumulated in the catholyte and then reached a stable concentration. Similar to the profile of the TAN change, that of the pH in the catholyte also increased rapidly and then remained stable, with pH values between 9.5 and 10.0 depending on the cathode operation mode, for all the systems (Fig. 6b). Because alkaline conditions were established in the catholyte, most of the NH_4^+-N transported from the synthetic wastewater to the catholyte was converted to free ammonia (Fig. 6c). By stripping, the free ammonia continuously entered the gas phase and finally accumulated in the absorption solution (Fig. 6d). After 72 h, the accumulation of NH_4^+-N in the absorption solution linearly increased for all the systems, and both the TAN concentration and pH of the catholyte remained stable, indicating that steady NH_4^+-N removal and recovery were achieved in all three systems.

The steady-state NH_4^+-N removal and recovery performances of the systems operated in different cathode modes are shown in Table 2. Under identical synthetic wastewater feeding conditions at the anode (450 mg NH_4^+-N L^{-1}, HRT = 12 h), a much higher NH_4^+-N removal efficiency was achieved in $S_{EM\text{-}1A}$ than in $S_{NonEM\text{-}1A}$ ($66.9 \pm 1.4\%$ vs. $18.5 \pm 1.3\%$). As expected, NH_4^+-N accumulated faster in the absorption solution in $S_{EM\text{-}1A}$ (Fig. 4d). Accordingly, the NH_4^+-N recovery rate in $S_{EM\text{-}1A}$ was calculated to be 6.9 ± 0.2 g N m^{-2} d^{-1}, which was 3.8 times higher than that in the $S_{NonEM\text{-}1A}$ system (1.8 ± 0.1 g N m^{-2} d^{-1}). The above results can be well explained by the higher current density in $S_{EM\text{-}1A}$ (as shown in Fig. 5a) and validated our hypothesis that the employment of tartrate-EDTA-Fe in the catholyte could promote NH_4^+-N recovery. In addition, as discussed in Section 3.2.1, the superiority of $S_{EM\text{-}1A}$ over $S_{NonEM\text{-}1A}$ was not only due to the elimination of the oxidizing equivalent supply limitation through the introduction of tartrate-EDTA-Fe, but also due to the better electrochemical performance obtained with tartrate-EDTA-Fe(III) as the electron acceptor instead of oxygen. Using the NH_4^+-N recovery rate obtained in $S_{NonEM\text{-}2A}$ (with a sufficient oxygen supply, 5.4 ± 0.3 g N m^{-2} d^{-1}) as an indicator, the contribution ratios of these two effects that promote NH_4^+-N recovery were 70.6% and 29.4%, respectively. Furthermore, by comparing the removal rates of NH_4^+-N with the recovery rates, the NH_4^+-N recovery efficiencies were calculated to be in the range of 85%–91% (as shown in Table 2), indicating that most of the removed NH_4^+-N was finally recovered into the absorption solution. Because the TAN concentration in the catholyte always remained stable in the steady operation stage (Fig. 6a), the small gap between the removed and recovered NH_4^+-N was likely due to some of the NH_4^+-N being removed via microbial assimilation at the bioanode instead being transported from the anode chamber to the cathode chamber [25]. Fig. 6a also shows that for the different cathode operation modes, the TAN concentration increased in the catholyte in the steady state and was stabilized at different levels, with that in $S_{EM\text{-}1A}$ being much higher. This was likely due to the high free ammonia concentration that had to be established in the catholyte in $S_{EM\text{-}1A}$ (as shown in Fig. 6c) to allow the ammonia stripping rate to match the high NH_4^+-N removal rate. In the case of $S_{NonEM\text{-}2A}$, although the NH_4^+-N removal rate was also much higher than that of $S_{NonEM\text{-}1A}$, the difference in the free ammonia concentration was not that significant. This result may be due to the introduction of an additional aeration point, which led to a higher flow rate of the stripping gas, another factor, in addition to the concentration of free ammonia, that positively correlates with the ammonia stripping rate [26].

3.3. Ammonia recovery performance at different ratios of the catholyte recirculation rate to the anolyte flow rate

As described in Section 3.2, when the ratio of the catholyte recirculation rate to the anolyte flow rate ($R_{C\text{-}A}$) was set to 12.0 and tartrate-EDTA-Fe was used, the oxidation equivalent supply rate was one order of magnitude higher than the consumption rate, indicating that $R_{C\text{-}A}$ should be reduced considerably to gain an energy benefit in $S_{EM\text{-}1A}$. As shown in Fig. 7a, the current density decreased when the $R_{C\text{-}A}$ was reduced to 1.0, and the decrease became more significant when $R_{C\text{-}A}$ was further halved. As expected, the variations in the NH_4^+-N recovery rates followed a similar trend as the current densities. Fig. 7b illustrates the supply rates and consumption rates of the oxidizing equivalent at different $R_{C\text{-}A}$ values. Using these two rates, we could estimate the ratio of Fe(III) to Fe(II) in the cathode chamber (details can be found in the SI), which is related to the cathode potential according to the Nernst equation. As shown in Fig. 7c, the ratio of Fe(III) to Fe(II) decreased with decreasing $R_{C\text{-}A}$, and the cathode potential followed

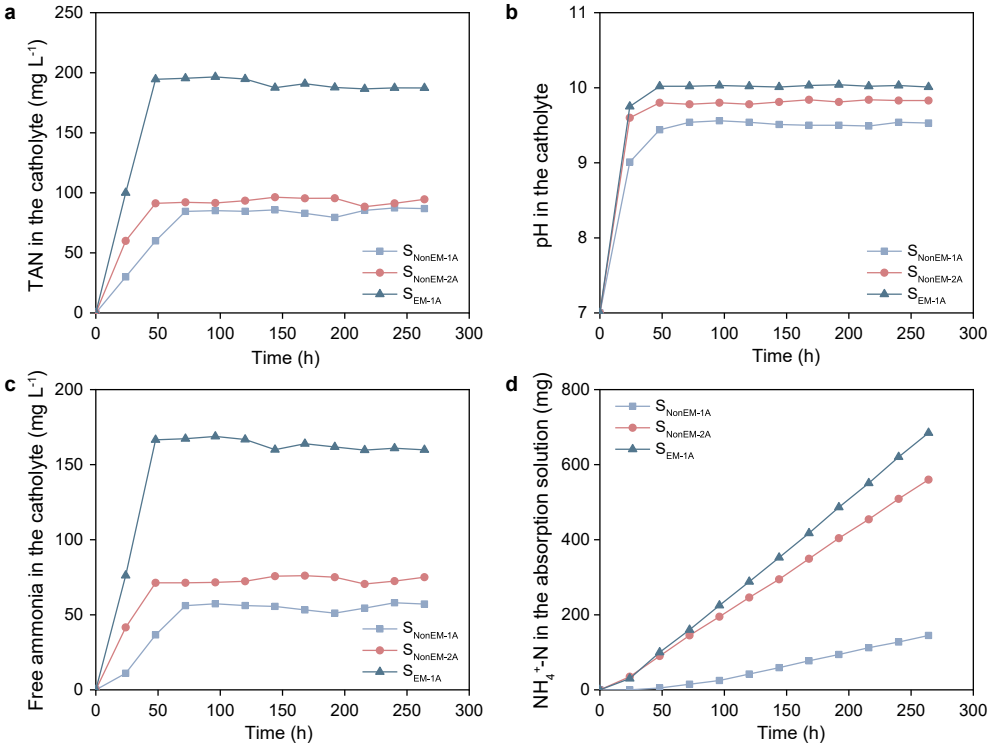

Fig. 6. Profiles of the TAN concentrations (**a**), pHs (**b**) and free ammonia concentrations (**c**) in the catholyte and of the recovered NH_4^+-N in the absorption solution (**d**) for systems with different cathode operation modes.

Table 2
NH_4^+-N removal and recovery performance in different cathode modes.

	Effluent NH_4^+-N (mg L^{-1})	N removal efficiency (%)	NH_4^+-N removal rate (g N m^{-2} d^{-1})	NH_4^+-N recovery rate (g N m^{-2} d^{-1})	N recovery efficiency (%)
$S_{NonEM-1A}$	367.29 ± 6.15	18.5 ± 1.3	2.1 ± 0.2	1.8 ± 0.1	85.0 ± 2.3
S_{EM-1A}	149.37 ± 6.23	66.9 ± 1.4	7.6 ± 0.2	6.9 ± 0.2	90.8 ± 2.5
$S_{NonEM-2A}$	205.45 ± 2.66	54.5 ± 0.7	6.2 ± 0.1	5.4 ± 0.3	88.1 ± 3.4

the same trend. As R_{C-A} was gradually decreased from 12.0 to 0.5, the cathode working potential decreased from −0.053 ± 0.008 V to −0.180 ± 0.004 V. Thus, the decline in the current density was caused by the negative shift in the cathode potential, which led to the deterioration of the abovementioned ammonia recovery performance. Nevertheless, the NH_4^+-N recovery rate of S_{EM-1A} at an extremely low R_{C-A} (4.2 ± 0.1 g N m^{-2} d^{-1}, $R_{C-A} = 0.5$) was still approximately 2.3 times higher than that obtained when the system was operating at a much higher R_{C-A} without tartrate-EDTA-Fe (1.8 ± 0.1 g N m^{-2} d^{-1}, $R_{C-A} = 12.0$ in $S_{NonEM-1A}$).

To further understand the energy budget, the energy consumption caused by catholyte recirculation was estimated (details can be found in the SI) and compared with the energy generation calculated from the current flowing across the resistance. As shown in Fig. 7d, at a relatively high R_{C-A} (12.0), the consumed energy was higher than the generated energy. In contrast, the energy consumption was significantly reduced at low R_{C-A} values and was much lower than the energy generation. In the same way, the energy profile of $S_{NonEM-1A}$, which has an awful budget, is also illustrated in Fig. 7d. These results clearly indicated that the introduction of tartrate-EDTA-Fe could allow the system to maintain a relatively high NH_4^+-N recovery performance at a low R_{C-A} while having a much better energy budget than the conventional system.

3.4. Perspectives

In this study, we showed that with the use of a tartrate-EDTA-Fe-amended catholyte, a higher ammonia recovery rate was achieved, and less energy was consumed than in the control system without the electron mediator. Previously, Sotres et al. reported a BES-stripping system similar to our control system but with a much higher R_{C-A} (288). However, the obtained ammonia recovery rate previously reported is still slightly lower than that achieved in our developed S_{EM-1A} with an extremely low R_{C-A} (0.5) (Table 3). This suggests that the superiority of the tartrate-EDTA-Fe-involved BES-stripping system over the conventional setup is not a case-dependent issue. As shown in Table 3, another BES operated in MFC mode had a similar ammonia recovery rate to the maximum achieved in S_{EM-1A} (7.1 ± 0.2 g N m^{-2} d^{-1} vs. 6.9 ± 0.2 g N m^{-2} d^{-1}). However, a noble metal catalyst was not used in the cathode in S_{EM-1A}, which is particularly promising for system scale-up and application because noble metal catalysts are the major contributor to the total capital cost of a BES [27].

In addition to capital expenditures, reliability is also an important factor that determines the application prospects of a technology. As shown in this work, the high ammonia recovery rate in the conventional setup relied on placing an additional aeration point in the cathode chamber to provide sufficient oxygen (Fig. 6 and Table 2, $S_{NonEM-2A}$ vs. $S_{NonEM-1A}$). In the case of system scale-up, a

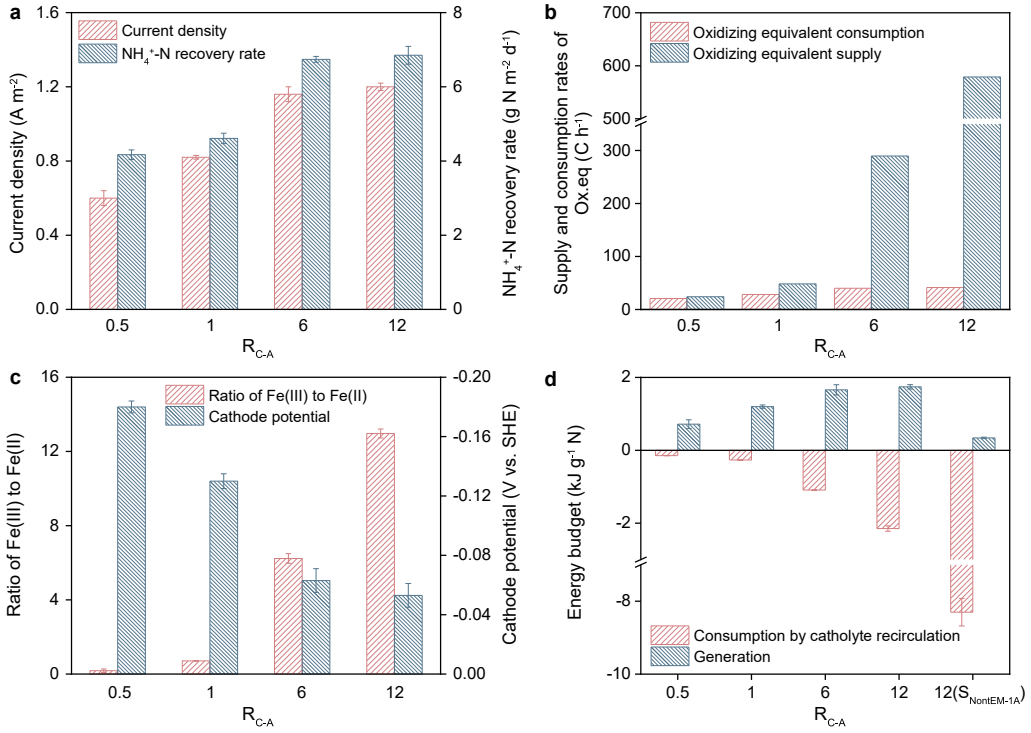

Fig. 7. Current densities and nitrogen recovery rates (**a**), supply and consumption rates of the oxidizing equivalent (Ox.eq) (**b**), ratios of Fe(III) to Fe(II) and cathode potentials (**c**) in S_{EM-1A} at different ratios of the catholyte recirculation rate to the anolyte flow rate (R_{C-A}), and the energy budgets of $S_{NonEM-1A}$ and S_{EM-1A} at different R_{C-A} (**d**).

Table 3
Comparison of the tartrate-EDTA-Fe-involved NH_4^+-N recovery system with previously reported studies.

Reactor type	Cathode side	NH_4^+-N recovery rate (g N m^{-2} d^{-1})	Catholyte recirculation ratio	Ref.
MFC with stripping column	Tartrate-EDTA-Fe as EM in catholyte	6.9 ± 0.2	12	This study
	Plain carbon brush as cathode	4.2 ± 0.1	0.5	
MFC with stripping column	No EM in catholyte	3.7 ± 0.2[a]	288	[3]
	Stainless steel mesh as cathode			
MFC- stripping	No EM in catholyte	7.1 ± 0.2	NA	[28]
	Pt-coated carbon cloth as cathode			
MEC (applied voltage 0.7 V)	Mixed metal oxide-coated titanium plate as cathode	27.0	NA	[9]

NA: Not available.
a: Assuming the recovery rate is equal to the reported removal rate.

number of additional aeration points should be used to meet the increase in the number of cathode chambers, and a complex gas tubing network should be added as well. In this way, the system reliability would be challenged by at least the following two aspects: (i) gas distribution from the air blower to each cathode chamber should be guaranteed; otherwise, an insufficient supply of oxygen to some cathodes would cause a decline in the ammonia recovery [28]; (ii) every connection of the gas tubing network should be well sealed; otherwise, the leakage of the aeration gas with ammonia would be dangerous and result in inefficient ammonia recovery. In comparison, our proposed novel system achieved a high ammonia recovery rate by placing the aeration point in the stripping column. The challenges mentioned above can be avoided by removing the air delivery points and corresponding collection system from the BES reactor, allowing the system to be applied at a large scale with high reliability.

Although the superiority of the BES-stripping system with an electron mediator over the conventional system has been verified here, there is still considerable room to further optimize this system. In this proof-of-concept work, the model EM employed was tartrate-EDTA-Fe, which has a redox potential of −0.075 V (vs. SHE, pH = 10). This potential is still far from the reduction potential of the terminal electron acceptor (oxygen, 0.627 V vs. SHE, at pH 10) [24]. Thus, it is expected that a higher ammonia recovery rate can be achieved by using an EM with a higher redox potential to promote current generation. Additionally, when selecting an EM with a higher redox potential, attention should also be paid to its oxidation kinetics. For instance, the redox couple of ferricyanide/ferrocyanide lies at a more positive redox potential (0.4 V vs. SHE, at pH 10) than tartrate-EDTA-Fe(III)/(III) [29], but the slow oxidation rate of ferrocyanide by oxygen disqualifies this redox couple as an EM in our proposed system. Efforts to seek or develop more efficient EMs are warranted in the future. Alternatively, as shown in Table 3, the BES operated in MEC mode with an applied voltage can also promote the ammonia recovery rate. Although this operation requires additional energy input, it could be a trade-off against capital expenditures, because a higher ammonia recovery rate could reduce the size of the BES reactor [30]. Notably, because the presence of the EM in the catholyte allows efficient transportation of the oxidizing equivalent from the stripping column to the cathode, the high current production in our proposed system may not rely on hydrogen evolution as in the conventional MEC. This will be

beneficial because the system can be more safely operated with less energy consumption.

4. Conclusions

In this work, a novel BES-stripping system was developed by introducing tartrate-EDTA-Fe into the catholyte as an electron mediator. With the aid of the tartrate-EDTA-Fe complex, the ammonia recovery rate increased by 3.8 times compared to that obtained without the EM. The improvement was attributed to the fact that using tartrate-EDTA-Fe provided an adequate oxidizing equivalent and improved the cathodic electrochemical performance. The contributions of these two effects accounted for 70.6% and 29.4%, respectively. In addition, the system with the electron mediator was obviously superior to the conventional system because it consumed less energy due to its lower catholyte recirculation rate compared with that of the conventional system. This study offers a strategy for scaling up BESs for ammonia recovery simply and reliably.

Declaration of interests

The authors declare that they have no known competing financial interests or personal relationships that could have appeared to influence the work reported in this paper.

Acknowledgments

This work was supported by the NSFC-EU Environmental Biotechnology joint program (No. 31861133001), Key Research and Development Project of Shandong Province (No. 2020CXGC011202), Shenzhen Science and Technology Program (No. KQTD20190929172630447) and China Postdoctoral Science Foundation (No. 2020M680708).

Appendix A. Supplementary data

Supplementary data to this article can be found online at https://doi.org/10.1016/j.ese.2022.100186.

References

[1] S.Y. Zhai, M. Ji, Y.X. Zhao, S.G. Pavlostathis, Biotransformation of 4-hydroxybenzoic acid under nitrate-reducing conditions in a MEC bioanode, Environ. Sci. Technol. 55 (3) (2021) 2067–2075.
[2] J.J. Wang, B.C. Huang, J. Li, R.C. Jin, Advances and challenges of sulfur-driven autotrophic denitrification (SDAD) for nitrogen removal, Chin. Chem. Lett. 31 (10) (2020) 2567–2574.
[3] A. Sotres, M. Cerrillo, M. Vinas, A. Bonmati, Nitrogen recovery from pig slurry in a two-chambered bioelectrochemical system, Bioresour. Technol. 194 (2015) 373–382.
[4] X. Wu, O. Modin, Ammonium recovery from reject water combined with hydrogen production in a bioelectrochemical reactor, Bioresour. Technol. 146 (2013) 530–536.
[5] Y.Y. Ye, H.H. Ngo, W.S. Guo, Y.W. Liu, S.W. Chang, D.D. Nguyen, H. Liang, J. Wang, A critical review on ammonium recovery from wastewater for sustainable wastewater management, Bioresour. Technol. 268 (2018) 749–758.
[6] B.E. Logan, D. Call, S. Cheng, H.V.M. Hamelers, T.H.J.A. Sleutels, A.W. Jeremiasse, R.A. Rozendal, Microbial electrolysis cells for high yield hydrogen gas production from organic matter, Environ. Sci. Technol. 42 (23) (2008) 8630–8640.
[7] R.A. Rozendal, H.V.M. Hamelers, K. Rabaey, J. Keller, C.J.N. Buisman, Towards practical implementation of bioelectrochemical wastewater treatment, Trends Biotechnol. 26 (8) (2008) 450–459.
[8] S. Gildemyn, A.K. Luther, S.J. Andersen, J. Desloover, K. Rabaey, Electrochemically and bioelectrochemically induced ammonium recovery, JoVE 95 (2015).
[9] P. Zamora, T. Georgieva, A. Ter Heijne, T.H.J.A. Sleutels, A.W. Jeremiasse, M. Saakes, C.J.N. Buisman, P. Kuntke, Ammonia recovery from urine in a scaled-up microbial electrolysis cell, J. Power Sources 356 (2017) 491–499.
[10] P. Kuntke, P. Zamora, M. Saakes, C.J.N. Buisman, H.V.M. Hamelers, Gas-permeable hydrophobic tubular membranes for ammonia recovery in bioelectrochemical systems, Environ. Sci.-Wat. Res. Technol. 2 (2) (2016) 261–265.
[11] Y.F. Zhang, I. Angelidaki, Submersible microbial desalination cell for simultaneous ammonia recovery and electricity production from anaerobic reactors containing high levels of ammonia, Bioresour. Technol. 177 (2015) 233–239.
[12] M. Cerrillo, M. Vinas, A. Bonmati, Overcoming organic and nitrogen overload in thermophilic anaerobic digestion of pig slurry by coupling a microbial electrolysis cell, Bioresour. Technol. 216 (2016) 362–372.
[13] J. Desloover, A.A. Woldeyohannis, W. Verstraete, N. Boon, K. Rabaey, Electrochemical resource recovery from digestate to prevent ammonia toxicity during anaerobic digestion, Environ. Sci. Technol. 46 (21) (2012) 12209–12216.
[14] A. Vilajeliu-Pons, S. Puig, I. Salcedo-Dávila, M.D. Balaguer, J. Colprim, Long-term assessment of six-stacked scaled-up MFCs treating swine manure with different electrode materials, Environ. Sci.: Water Res. Technol. 3 (5) (2017) 947–959.
[15] A.J. Wang, H.C. Wang, H.Y. Cheng, B. Liang, W.Z. Liu, J.L. Han, B. Zhang, S.S. Wang, Electrochemistry-stimulated environmental bioremediation: development of applicable modular electrode and system scale-up, Environ. Sci. Ecotechnol. 3 (2020), 100050.
[16] D.C. Schiavon Maia, R.R. Niklevicz, R. Arioli, L.M. Frare, P.A. Arroyo, M.L. Gimenes, N.C. Pereira, Removal of H_2S and CO_2 from biogas in bench scale and the pilot scale using a regenerable Fe-EDTA solution, Renew. Energy 109 (2017) 188–194.
[17] K. Shimizu, R. Hutcheson, M.D. Engelmann, I.F. Cheng, Cyclic voltammetric and aqueous equilibria model study of the pH dependant iron(II/III)ethylenediamminetetraacetate complex reduction potential, J. Electroanal. Chem. 603 (1) (2007) 44–50.
[18] L.F. Deng, C.G. Zhou, J.T. Zhang, L. Zhuang, N. Lu, L.X. Zhang, Sustainable electricity generation in microbial fuel cells using Fe(III)-EDTA as cathodic electron shuttle, Environ. Sci. 30 (2009) 2142–2147.
[19] C.W. Edmunds, C. Hamilton, K. Kim, S.C. Chmely, N. Labbé, Using a chelating agent to generate low ash bioenergy feedstock, Biomass Bioenergy 96 (2017) 12–18.
[20] V. Salvado, X. Ribas, M. Valiente, The chemistry of iron in biosystems-V study of complex formation between iron(III) and tartaric acid in alkaline aqueous solutions, Talanta 39 (1992) 73–76.
[21] H.Y. Cheng, B. Liang, Y. Mu, M.H. Cui, K. Li, W.M. Wu, A.J. Wang, Stimulation of oxygen to bioanode for energy recovery from recalcitrant organic matter aniline in microbial fuel cells (MFCs), Water Res. 81 (2015) 72–83.
[22] S.Y. Sun, Y.N. Hou, W. Wei, H.M.A. Sharif, C. Huang, B.J. Ni, H.B. Li, Y.Y. Song, C.C. Lu, Y. Han, J.B. Guo, Perturbation of clopyralid on bio-denitrification and nitrite accumulation: long-term performance and biological mechanism, Environ. Sci. Ecotechnol. 9 (2022), 100144.
[23] H.Y. Cheng, X.D. Tian, C.H. Li, S.S. Wang, S.G. Su, H.C. Wang, B. Zhang, H.M.A. Sharif, A.J. Wang, Microbial photoelectrotrophic denitrification as a sustainable and efficient way for reducing nitrate to nitrogen, Environ. Sci. Technol. 51 (21) (2017) 12948–12955.
[24] B.E. Logan, B. Hamelers, R. Rozendal, U. Schrorder, J. Keller, S. Freguia, P. Aelterman, W. Verstraete, K. Rabaey, Microbial fuel cells: methodology and technology, Environ. Sci. Technol. 40 (17) (2006) 5181–5192.
[25] M. Villano, S. Scardala, F. Aulenta, M. Majone, Carbon and nitrogen removal and enhanced methane production in a microbial electrolysis cell, Bioresour. Technol. 130 (2013) 366–371.
[26] B.X. Liu, A. Giannis, J.F. Zhang, V.W.C. Chang, J.Y. Wang, Air stripping process for ammonia recovery from source-separated urine: modeling and optimization, J. Chem. Technol. Biotechnol. 90 (12) (2015) 2208–2217.
[27] A. AlSayed, M. Soliman, A. Eldyasti, Microbial fuel cells for municipal wastewater treatment: from technology fundamentals to full-scale development, Renew. Sustain. Energy Rev. 134 (2020).
[28] M.H. Qin, Y. Liu, S. Luo, R. Qiao, Z. He, Integrated experimental and modeling evaluation of energy consumption for ammonia recovery in bioelectrochemical systems, Chem. Eng. J. 327 (2017) 924–931.
[29] J.E. O'Reilly, Oxidation-reduction potential of the ferro-ferricyanide system in buffer solutions, Biochim. Biophys. Acta Bioenerg. 292 (3) (1973) 509–515.
[30] H.C. Wang, H.Y. Cheng, D. Cui, B. Zhang, S.S. Wang, J.L. Han, S.G. Su, R. Chen, A.J. Wang, Corrugated stainless-steel mesh as a simple engineerable electrode module in bio-electrochemical system: hydrodynamics and the effects on decolorization performance, J. Hazard Mater. 338 (2017) 287–295.